Quantifying the soil sink of atmospheric Hydrogen: a full year of field measurements from grassland and forest soils in the UK

Nicholas Cowan[1], Toby Roberts[1], Mark Hanlon[1], Aurelia Bezanger[1], Galina Toteva[1,2], Alex Tweedie[1,2], Karen Yeung[1], Ajinkya Deshpande[1], Peter Levy[1], Ute Skiba [1], Eiko Nemitz[1], Julia Drewer[1]

[1]UK Centre for Ecology and Hydrology, Easter Bush, Midlothian, UK, EH26 0QB

[2]School of GeoSciences, The University of Edinburgh, Edinburgh, United Kingdom

Corresponding author: Nicholas Cowan (nicwan11@ceh.ac.uk)

Keywords: greenhouse gas, carbon, methane, flux, chamber methodology

Abstract

Emissions of hydrogen (H_2) gas from human activities are associated with indirect climate warming effects. As the hydrogen economy expands globally (e.g. the use of H_2 gas as ~~an energy source~~a fuel), the anthropogenic release of H_2 into the atmosphere is expected to rise rapidly as a result of increased leakage. The dominant H_2 removal process is uptake into soils; however, removal mechanisms are poorly understood and the fate and impact of increased H_2 emissions remains highly uncertain. Fluxes of H_2 within soils are rarely measured, and data to inform global models is based on few studies. This study presents soil H_2 fluxes from two field sites in central Scotland, a managed grassland and a planted deciduous woodland, with flux measurements of H_2 covering full seasonal cycles. A bespoke flux chamber measurement protocol was developed to deal with the fast decline in headspace concentrations associated with rapid H_2 fluxes, in which ~~non-linear~~exponential regression models could be fitted to concentration data over a 7-minute enclosure time. We estimate annual H_2 uptake of -3.1 ± 0.1 and -12.0 ± 0.4 kg H_2 ha^{-1} yr^{-1} and mean deposition velocities of 0.012 ± 0.002 and 0.088 ± 0.005 cm s^{-1} for the grassland and woodland sites, respectively. Soil moisture was found to be the primary driver of H_2 uptake at the grassland site, where the high silt/clay content of the soil resulted in anaerobic conditions (near zero H_2 flux) during wet periods of the year. Uptake of H_2 at the forest site was highly variable and did not correlate well with any localised soil properties (soil moisture, temperature, total carbon and nitrogen content). It is likely that the high silt/clay content of the grassland site (55% ~~clay~~silt, 20% clay) decreased aeration when soils were wet, resulting in poor aeration and low H_2 uptake. The well-drained forest site (~~25~~60% ~~clay~~sand) was not as restricted by exchange of H_2 between the atmosphere and the soil, showing instead a large variability in H_2 flux that is more likely to be related to heterogeneous factors in the soil that control microbial activity (e.g. labile carbon and microbial densities).

The results of this study highlight that there is still much that we do not understand regarding the drivers of H_2 uptake in soils and that further field measurements are required to improve global models.

1. Introduction

Prior to the industrial revolution in the 18th century, the atmospheric concentration of Hydrogen gas (H_2) was relatively stable at approximately 330 ppb (Patterson et al., 2021). Human activity over the past two centuries has resulted in increasing atmospheric H_2 concentrations (546 ppb in 2021, Petron et al. (2023)), partly as a result of increasing industrial leaks (Hitchcock 2019; Cooper et al., 2022), partly due to increases in emissions and concentrations of precursor gases such as methane (CH_4) and volatile organic compounds (VOCs), and partly due to increasing concentrations of other gases in the atmosphere which extend the natural lifetime of H_2 (Patterson et al., 2021). In the atmosphere, H_2 competes for hydroxyl (OH) radicals with gases such as methane (CH_4) and carbon monoxide (CO), thus an increase in concentrations of these gases due to human activities has resulted in increasing competition for OH and extended the lifetimes for each species (Khalil & Rasmussen, 1990; Bertagni et al., 2022). Concentrations of atmospheric H_2 gas are indirectly associated with climate warming effects as a result of extending the atmospheric lifetime of the powerful greenhouse gas CH_4 as well as increasing tropospheric ozone and stratospheric water vapour, which also have a warming potential (Warwick et al., 2004; Ocko & Hamburg, 2022). The associated indirect global warming potential (GWP) had been estimated to be in the range of 3.3 to 5 over a hundred-year time horizon (Derwent et al., 2020, Field & Derwent, 2021), though recent estimates have been made of up to 11.6 ± 2.8 times that of an equivalent mass of carbon dioxide (Sand et al., 2023). The effective GWP and the atmospheric accumulation of H_2 are highly sensitive to its atmospheric lifetime, which is estimated to be approximately 2 years (Novelli et al., 1999).

The dominant process for H_2 removal from the atmosphere is uptake by soils, which is estimated to be three times larger than the sink due to atmospheric reaction with OH (Warwick et al., 2004; Derwent et al., 2020; Field & Derwent, 2021; Paulot et al., 2021; Ocko & Hamburg, 2022). Whilst both removal mechanisms are highly uncertain (especially the soil sink), the fate and impact of increased H_2 emissions depends largely on the soil sink strength (Ehhalt & Rohrer, 2009). The ~~soil H_2 sink~~microbial uptake of H_2 ~~is~~ can occur ~~caused by microbial activity,~~ both under aerobic and anaerobic conditions, but the global atmospheric H_2 sink is dominated by processes that occur in aerobic soils at the atmosphere-biosphere interface (soil surface) where atmospheric H_2 availability is not as limited (Piché-Choquette & Constant, 2019). A large spectrum of bacteria and archaea can utilise H_2 as an energy source, via the hydrogenase enzyme. Whilst some investigations have highlighted the importance of high-affinity H_2-oxidising bacteria (Saavedra-Lavoie et al., 2020), most studies suggest that this enzyme is widespread across many bacterial and archaeal phyla, and that H_2 consumption

Formatted: Subscript

Formatted: Subscript

is the norm rather than the exception (Islam et al., 2020; Greening & Grinter, 2022). ~~It has been suggested that the potential soil H_2 sink is very large because of the high H_2 demand of microbes (Smith-Downey et al., 2008). However,~~ Studies investigating specific H_2 uptake rates for different soil types and conditions ~~are lacking~~have been carried out but are sparse and limited to a small number of geographies (primarily North America, Europe and Japan, e.g., Yonemura et al., 1999; Yonemura et al., 2000; Smith-Downey 2008; Lallo et al., 2009; Hammer and Levin, 2009; Khdhiri et al., 2015). In addition to microbial activity, diffusion into the soil is a further important rate limiting step (Bertagni et al., 2021). Gases penetrate the soil by passive diffusion and diffusion rates are mainly influenced by porosity, which is affected by soil structure, texture, organic matter contents, vegetation types (roots) and moisture content. Thus, for the same microbial activity, porous soils can be expected to be much larger H_2 sinks than compacted and/or waterlogged soils due to increased gas exchange rates with the atmosphere. At the larger scale, diffusion rates will depend on the changing climate: a wetter climate may lower the H_2 diffusion rates (Paulot et al., 2021). Temperature is another important factor as it determines the rate of microbial enzyme reactions, ~~and~~ in addition a carbon source is also required for heterotrophic microbial activity (Islam et al., 2020; Meredith et al., 2016; Baril et al., 2022). ~~In addition, soil H_2 concentrations will be competing with CH_4 as the energy source for soil microbes, hence the H_2 sink strength may in turn affect the CH_4 sink strength and vice versa (Conrad, 1999).~~ The biological sink of atmospheric H_2 has been suggested to be more sensitive to spatial variations of drivers (specifically microbial diversity) compared to the fluxes of other gases with high variability such as nitrous oxide (N_2O) (e.g. Baril et al., 2022); however, studies reporting the spatial variability of H_2 ~~measurement data~~ fluxes in soils are limited ~~limited (Baril et al., 2022)~~.

Historically, the processes that control H_2 uptake in soils have been severely understudied due to the logistical difficulties and technical constraints on measuring H_2 fluxes. This study presents measurements of H_2 fluxes between the soil and the atmosphere at two field sites in central Scotland, a managed grassland and a planted deciduous woodland. These are the first reported flux measurements of H_2 covering a full annual cycle in the UK. It has previously been reported that forest ecosystems exhibit higher H_2 uptake rates than agroecosystems (Ehhalt and Rohrer, 2009); however, the generality of this and exact mechanisms are still unclear. This study aims to investigate the response of microbial H_2 uptake at a grassland and a forest site to environmental drivers, and to identify differences between the sites. We also describe a dedicated flux chamber methodology which has been developed to best address the challenges of measuring H_2 flux using gas chromatography (GC) analysers.

2. Methods

2.1. Field Sites

Measurements of trace gas fluxes and environmental variables were made at two field sites within the Midlothian region in central Scotland (UK, approximately 6 miles south of Edinburgh, Table 1). The first of these was the long-term environmental monitoring site at Easter Bush Farm (grassland). The grassland site (55.8653 °N, -3.206 °W) is an intensively managed, improved grassland (South field in Cowan et al., 2020 and Drewer et al., 2016) that since 2001 has been used predominantly to graze sheep, with a species composition of >99% perennial ryegrass (*Lolium perenne*). The soil type is an imperfectly drained Eutric Cambisol with ~~clay~~ silt loam soil. The field management is typical for this region, with predominately ammonium nitrate (AN) fertilisation via tractor-mounted broadcast spreading, with liming every 3 – 5 years to maintain the pH between 5.5 and 6.0 and occasional ploughing and reseeding. The sheep were absent from the fields in the winter months (November to February), with sporadic movement between local fields throughout the growing season (March to September) as management required. During the period of 01/10/23 to 01/10/24, the cumulative rainfall at the grassland site was 1133 mm and the mean temperature was 8.6 °C which is fairly typical of the site (Table 1)

The second field site was a temporary experimental area setup in Glencorse Forest (woodland). Glencorse Forest (55.8540°N, -3.215°W) was converted to a planted deciduous forest from a pasture approximately 40 years prior to measurements (Billington and Pelham, 1991). The study plot is situated in a plantation of Silver Birch (*Betula pendula*) and Downy Birch (*Betula pubescens*), with a ground flora consisting mostly of grasses. The soil is classified as a sandy loam which lies under a thin layer (5 – 10 mm) of organic debris. The field site had been subject to enhanced nitrogen deposition with ammonia for approximately 2 years before H_2 flux measurements were carried out (Deshpande et al., 2024). During the period of 01/10/23 to 01/10/24, the cumulative rainfall at the woodland site was 1047 mm and the mean temperature was 9.6 °C which was slightly wetter and warmer than historical mean data (Table 1).

Table 1 Field site environmental properties as reported in previous studies and ongoing research. Mean annual values taken from 10+ years of site data. Rainfall represents throughfall (e.g. rain that reaches the soil).

Property	**Easter Bush Farm**	**Glencorse Forest**
Management	Improved grassland (grazed)	Planted woodland (Birch)
Abbreviation	Grassland	Woodland
Soil Type	Mineral	Mineral
Carbon Content (% mass)	4.0	3.1
pH	5.5	5.3
Bulk Density (g cm^{-3})	1.11	0.96
Particle Density (g cm^{-3})	2.57	2.34

Sand/silt/clay (%)	25/~~20~~55/~~55~~20	60/15/25
Mean Annual Temperature (°C)	8.4	9.0
Mean Annual Rainfall (mm)	1040	920

2.2. *Meteorological and soil measurements*

Continuous environmental measurements were made at both field sites. Air temperature, soil temperature, soil volumetric water content (VWC) at three depths (5, 10 and 20 cm at the grassland site; 5, 10 and 15 cm at the woodland site), relative humidity (RH) and rainfall were measured at both sites throughout the flux measurement campaign (Table S1). For each flux chamber measurement, soil temperature and soil VWC were also measured next to the chamber (<0.5 m distance) at the time of the flux measurement. Soil temperature was measured at 10 cm depth using a handheld probe (ETI Ltd., Worthing, UK), and soil VWC was measured at 12 cm depth using an HS2 HydroSense II handheld soil moisture sensor (Campbell Scientific, Utah, USA), with 4 replicates for each chamber. Soil samples were collected for total carbon (C) and total nitrogen (N) analysis from the top 10 cm of soil at the woodland site in March 2021, September 2021, May 2022, August 2022, November 2022, and March 2023. Subsamples were dried at 105 °C until constant weight, milled using a ball mill (MM200 ball mill, Retsch, Haan, Germany) and analysed using an elemental analyser (Flash SMART, Thermo Fisher Scientific, MA, USA).

2.3. *Flux measurements*

Fluxes of hydrogen (H_2), methane (CH_4) and nitrous oxide (N_2O) were measured using the static chamber method (e.g. Drewer et al., 2016). Chambers (diameter = 40 cm, height = 30 cm) consisting of opaque polypropylene open-ended cylinders, were installed at each field site: 20 at Easter Bush (grassland) and 36 at Glencorse (woodland). The chambers were inserted into the ground to a depth of approximately 10 cm for the entire study period (chamber air volume of approximately 0.025 m^3). The depth to the surface in each chamber was measured at 5 points on the sides of the chamber base using a ruler, from which the average was used to calculate the volume of air within. During measurement periods, aluminium lids were fastened onto the bases using four strong clips; a strip of draft excluder glued onto the lid provided a gas tight seal between chamber and lid. A three-way tap was used for gas sample removal using a 100 ml syringe. 20 ml glass vials were filled with a double needle system to flush the vials with five times their volume. Storage tests using gas standards revealed that gases stored in the vials were stable for up to 24 hours, after which H_2 leakage could be observed in the data. Hence all analyses of H_2 gas samples from the chambers were carried

Formatted: Superscript

out within 24 hours of measurement in the field (typically within 6 hours). Measurements of H_2 and GHGs were made approximately monthly.

Two separate measurement protocols were employed to measure greenhouse gases (GHGs) and H_2 fluxes, due to the differences in how the gases behaved within the chamber over a given timespan. For GHG measurements, the standard practice of extracting four gas samples (100 ml) at regular intervals over one hour (0, 20, 40, 60 min) was used (Drewer et al. 2017). However, due to the rapid uptake of H_2 observed in trial measurements (H_2 in the chamber headspace could reach zero ppb in under 10 mins), the time-evolution of H_2 in the chamber was non-linear and therefore a separate measurement protocol was developed for H_2 fluxes. Fluxes of H_2 were measured during entirely separate enclosure periods to the GHGs (albeit on the same day) using an enclosure period with 6 samples taken over 7 minutes (0, 1, 2, 3, 5 & 7 mins). Chambers used to measure H_2 were fitted with a small 5 cm diameter PC fan which ran from a 9 V battery during chamber enclosure times to ensure rapid air mixing over the shorter measurement period.

Concentrations of H_2 were measured using an Agilent 8890 gas chromatograph fitted with a pulsed discharge helium ionization detector (GC-PDHID) equipped with a 7697A headspace autosampler, with capacity for 108 vials (Agilent, Santa Clara, California, USA). Concentrations of CH_4 and N_2O were measured using a gas chromatograph (Agilent 7890B with headspace autosampler 7697A with capacity for 108 vials; Agilent, Santa Clara, California, USA) with a micro-electron capture detector (µECD) for N_2O analysis and flame ionization detector (FID) for CH_4 analysis run in parallel. Each analytical run of H_2 and GHG samples included at least three sets of four certified standard concentrations for calibration purposes (certified to ± 5%). The instrumental noise (σ) of the instruments were 40, 5, and 15 ppb for CH_4, N_2O and H_2, respectively. Based on the methods used, the analytical uncertainty in flux estimates were 0.~~38~~55, 0.~~047~~ 07 and 1.~~08~~ 0 nmol m^{-2} sec^{-1} for CH_4, N_2O and H_2, respectively based on the method of Cowan et al. (2025).

Fluxes were calculated using linear and non-linear regression methods using the HMR package for the statistical software R (Pedersen *et al.*, 2010). By convention, positive fluxes represent emission from the soil, and negative fluxes indicate that the soil acts as a sink (i.e. uptake). Fluxes of GHGs were all calculated using linear regression, where *dC/dt* is calculated using the standard line of best fit through the concentration data. As concentrations of H_2 fall exponentially during chamber measurements when soil uptake of H_2 is high, linear regression is not always appropriate. To account for this, fluxes of H_2 were calculated using both linear regression and the HMR model, depending on the magnitude of the rate of change observed in each chamber measurement. The HMR model is a commonly used non-linear model derived by Hutchinson & Mosier (1981) with a negative exponential form of curvature which calculates the rate of change of a gas concentration at $t = 0$. The concentration C at time t is given by Equation 1, where C_0 is the initial concentration, ~~C_{max}~~ C_{eq} is the

value at equilibrium and *k* is a constant. *dC/dt* is the initial rate of change in concentration at *t* = 0 in nmol mol^{-1} s^{-1}, calculated using Equation 2.

$$C_t = C_{maxeq} - \left(C_{eqmax} - C_o\right)\exp(-kt) \quad \text{(Equation 1)}$$

$$\frac{dC}{dt} = k(C_{eqmax} - C_o) \quad \text{(Equation 2)}$$

The *dC/dt* at t=0 is used to calculate the flux using Equation 3, where *F* is gas flux from the soil (nmol m^{-2} s^{-1}), ρ is the density of air in mol m^{-3}, *V* is the volume of the chamber in m^3 and *A* is the ground area enclosed by the chamber in m^2.

$$F = \frac{dC}{dt} \times \rho \times \frac{V}{A} \quad \text{(Equation 3)}$$

~~At low concentrations near the limit of detection of the analyser~~Where soil flux is near the analytical uncertainty of the method (e.g. concentration change within the chamber is difficult to detect with our instrument), a clear exponential decline was hard to discern from the measurement noise and could give rise to spurious fits to Equation 1. (Examples 1 and 2 in Figure 1 and Table 2). The criteria for using the HMR model for each individual flux calculation was based on i) *k* is not unrealistically large in Equation 2 (as defined and limited by the HMR package in R), ii) the flux estimated by linear regression is larger than the analytical uncertainty of the method (1.~~08~~ 0 nmol m^{-2} s^{-1} for H_2) and iii) the 95 % confidence interval (95% C.I.) of the HMR model fit is less than 5 times the magnitude of the flux estimated using linear regression (removes poor-fitting outliers). In Figure 1 and Table 3, six examples are given in which three selections of linear regression fitting and three selections of the HMR model fitting are used to determine flux. For large uptake fluxes (Examples 4, 5 and 6) the HMR model provides a more suitable fit to the non-linearity in *dC*/*dt*, which linear regression does not accurately represent. Deposition velocity of H_2 was calculated by dividing the calculated flux by the ambient concentration at the site (mean of *t* = 0 measurements on day of measurement in mol m^{-3}).

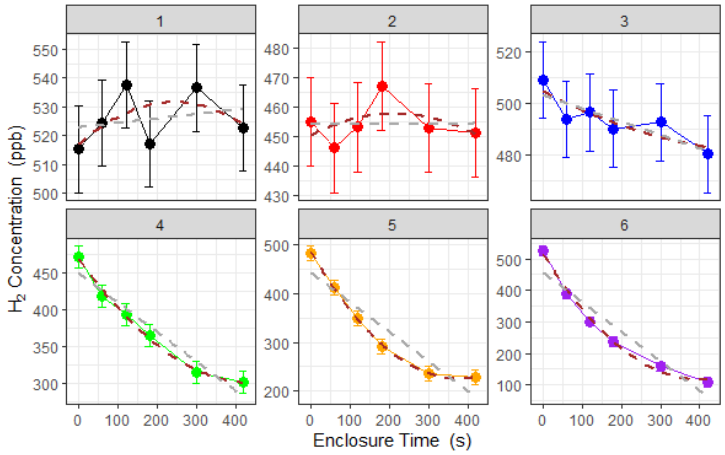

Figure 1. Examples of concentration data collected during H_2 flux chamber sampling. Linear regression (grey) and HM model (brown) are used to determine *dC*/*dt* for each chamber measurement. Error bars represent the ~~analytical uncertainty~~instrumental noise of H_2 measurements ~~by~~ in GC analysis (15 ppb in this study). Comparisons of flux data presented in Table 2.

Table 2. Further information on the example data provided in Figure 1. Six examples of chamber H_2 flux measurements are provided, from the Easter Bush (grassland) and Glencorse (woodland) field sites. The initial and final concentrations of H_2 within the chamber are provided, as well as the flux and 95% C.I. calculated using linear and HM model (Equation 2) fitting methods (NA when *k* is too large). The method selected to represent the flux in this study based on the described protocols is included.

Example	Date	Location	Initial (ppb)	Final (ppb)	Flux Linear fit (nmol m^{-2} s^{-1})	Flux HM fit (nmol m^{-2} s^{-1})	Selected Method
1	10/04/2024	Grassland	515	522	0.01 (-0.59 – 0.63)	2.839 (NA)	Linear
2	16/11/2023	Grassland	455	451	0.003 (-0.56 – 0.60)	0.239 (-6.47 – 6.99)	Linear
3	13/02/2024	Grassland	509	480	-0.319 (-0.58 – -0.06)	-0.889 (-2.60 – 0.21)	Linear
4	31/07/2024	Grassland	471	300	-3.078 (-4.54 – -3.35)	-6.6 (-9.44 – -3.80)	HM
5	31/07/2024	Grassland	483	229	-3.152 (-4.54 – -3.35)	-10.89 (-15.54 – -6.232)	HM
6	04/04/2024	Woodland	527	109	-5.278 (-7.05 – -1.07)	-14.35 (-15.88 – -12.82)	HM

3. Results

3.1. Hydrogen Flux measurements

Fluxes of H_2 measured from the grassland site ranged from -15.5 to +5.3 nmol m^{-2} s^{-1} ~~(deposition velocity (Vd) ranged from 0.070 to -0.026 cm s^{-1})~~ (Figures 2 and S1) over the period of September 2023 to September 2024. More than 90% of the H_2 fluxes measured at the grassland site were negative (soil uptake) and only 2 of 251 chamber measurements showed emissions from the soil which exceed the analytical uncertainty of the method. Fluxes of H_2 at the grassland site changed seasonally, with greater uptake in the spring and summer compared with winter, where the flux was close to zero. Fluxes at the grassland site had a median of -1.2 nmol m^{-2} s^{-1} and 95% percentiles of -9.9 to 0.2 nmol m^{-2} s^{-1}. Fluxes measured from the woodland site ranged from -40.7 to -1.1 nmol m^{-2} s^{-1} ~~(Vd ranged from 0.191 to 0.005 cm s^{-1})~~ (Figures 2 and S1). All fluxes measured at the woodland site showed H_2 uptake in the soil. Spatial variability of H_2 flux at the woodland site was an order of magnitude larger than those observed at the grassland site. Fluxes at the woodland site had a median of -18.7 nmol m^{-2} s^{-1} and 95% percentiles of -32.4 to -4.3 nmol m^{-2} s^{-1}. Ambient concentrations of H_2 at the sites ranged from 424.8 to 566.5 ppb. Mean ambient concentrations at the woodland site (484.4 ppb) were on average 21.7 ppb (4.3 %) lower than the grassland site (506.5 ppb) which could be considered statistically insignificant (t-test, $p > 0.1$), but differences were fairly consistent throughout the year (summary statistics presented in Table S2).

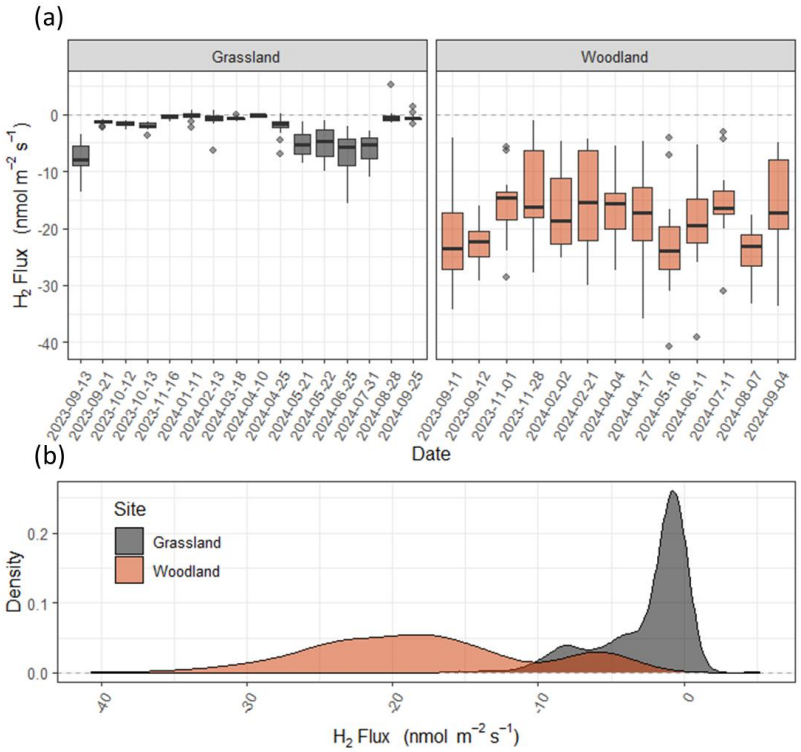

Figure 2. Fluxes of H_2 measured using the flux chamber method at grassland (Easter Bush, grassland; grey) and forest (Glencorse Forest, woodland; red) sites in Midlothian, Scotland. Boxplots (a) represent the median, and 25th and 75th percentiles of flux data of 20 chambers, respectively (whiskers represent the 95th percentiles). (b) Frequency distributions of the flux data for both sites (Figure replicated for Vd in Figure S1).

3.2. Greenhouse gas fluxes

Fluxes of CH_4 at both sites were close to zero, with mostly small negative fluxes observed at both sites (Figure S3). Soil uptake of CH_4 was observed during the summer months at both sites but during colder months, only the woodland site continued to observe consistent negative CH_4 fluxes. Fluxes of CH_4 measured from the grassland site ranged from -1.2 to 1.0 nmol m^{-2} s^{-1} with a median of -0.14 nmol m^{-2} s^{-1}. Fluxes of CH_4 measured from the woodland site ranged from -1.3 to 2.3 nmol m^{-2} s^{-1} with a median of -0.32 nmol m^{-2} s^{-1}. Only 40% of all CH_4 flux measurements exceeded the analytical uncertainty of the chamber method deployed, highlighting the magnitude of observed fluxes were near the limit of detection of the methodology. Fluxes of N_2O measured at both sites were relatively low for all measurement dates (58% of all data below the analytical

uncertainty) with the exception of measurements made in April at the grassland site. Nitrogen fertiliser was applied to the field on the 28th of March, resulting in increased N_2O emissions for several weeks (Figure S3).

3.3. *Drivers of H_2 flux*

Correlations of H_2 flux with soil moisture and soil temperature can be observed at both sites (Figures 4a, ~~&~~ 4b and S4); however, each site responds differently. Fluxes of H_2 at the grassland site were close to zero when water filled pore space (WFPS) was high (>45%), then tended towards uptake as WFPS decreased. The correlation between H_2 flux and WFPS is weaker at the woodland site and flux data are widely scattered. Fluxes of H_2 at both the grassland and woodland site tended towards higher uptake as temperature increased, though scatter increased toward higher uptake at both sites (>12 °C). A simplistic multiple regression fit between H_2 flux (y) with soil moisture (x) and soil temperature (z) ($y = a_1x^2 + a_2x + b_1z^2 + b_2z + c$) accounts for more than half of the variance in the observed fluxes at the grassland site (R^2 = 0.60) with a significant contribution from soil moisture, but the same approach does not adequately represent the large flux variability at the woodland site (R^2 = 0.14) for which neither soil moisture or soil temperature was found to correlate significantly (Table S3). Fluxes of CH_4 at the sites followed the same trends as H_2 flux in terms of emission/uptake and follow similar correlations with soil moisture and soil temperature as H_2 flux (Figures 4c & 4d). Fluxes of CH_4 at both sites were close to zero (or emission) when soils were wet (>45 % WFPS) and cold (<6 °C). Uptake of CH_4 was greatest when soils were drier and warm.

~~Total carbon (C) and total nitrogen (N) from the woodland site provided comparisons of H_2 flux with soil C and N at the chamber level (Figure S4).~~ No correlation between H_2 flux with measured total soil C or N in the top 10 cm was found at the woodland site (R^2 < 0.01 for each) (Figure S5). Variability in C and N in the replicated cores ~~per~~ in the soils in the vicinity of each chamber (< 1 m^2 distance) ~~chamber~~ was similar to the magnitude of spatial variability observed at the entire plot scale. This suggested a relatively large variability in the soil C and N content at small scales which may obfuscate correlation between soils and fluxes at the individual chamber scale (destructive sampling could not be carried out on soil within the chambers without invalidating flux measurements). ~~, suggesting that localised soil samples were not adequately representative of the soil within a chamber (high spatial variability of C and N in the soil at the <1 m^2 scale). No correlation between H_2 flux with measured total soil C or N in the top 10 cm was found at the woodland site (R^2 < 0.01 for each).~~

By combining continuous soil measurement data collected at each site (soil moisture and temperature at 10 cm depth), with the multiple regression model with soil moisture and soil temperature (Figures 4b & 4c) as described in Table S1, continuous H_2 flux predictions were made for a full year (Figure 4a). This model predicts that H_2 flux at the grassland site remains close to zero for most of the time, except when soil moisture drops

Formatted: Superscript

(e.g. warm months in spring and summer). The model predicts that H_2 flux at the grassland site is strongly dependent on the soil moisture content, with relatively strong periods of H_2 uptake during drier periods (warm periods between rainfall events). H_2 flux estimates at the woodland site are more variable, and less susceptible to changes in meteorology or soil conditions. The model predicts a slowdown in H_2 uptake in the forest soils during the colder months in winter but is not significantly impacted by changing soil moisture. Total annual estimates of H_2 flux predicted by the model are -3.1 ± 0.1 and -12.0 ± 0.4 kg H_2 ha^{-1} yr^{-1} for the grassland and woodland sites, respectively. By comparison, a straight average of the measurements, without using models to gap-fill the data, suggests mean fluxes (with 95% C.I.s) of -2.6 ± 0.4 and -18.7 ± 1.0 nmol m^{-2} s^{-1} which would translate to annual cumulative fluxes of approximately -1.6 ± 0.2 and -11.7 ± 0.6 kg H_2 ha^{-1} yr^{-1} for the grassland and GC sites, respectively. The two estimates agree well at the woodland site, but the gap filling increases the estimated annual H_2 uptake at the grassland site by 56%.

290

291

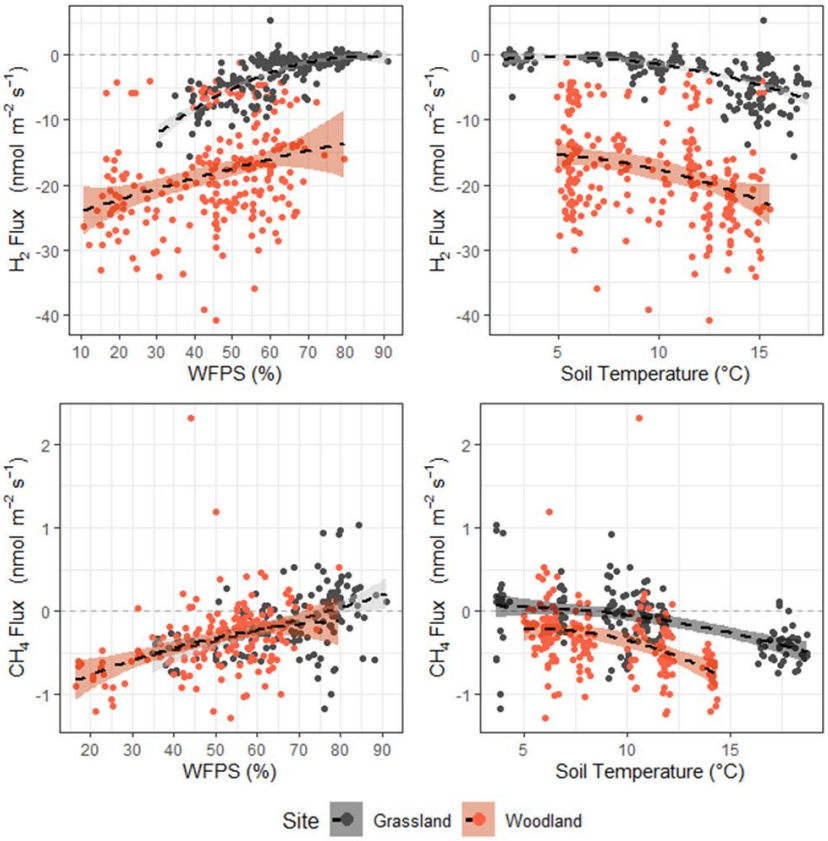
H_2 Flux (nmol m^{-2} s^{-1})
0
-10
-20
-30
-40
10 20 30 40 50 60 70 80 90
WFPS (%)
5 10 15
Soil Temperature (°C)
CH_4 Flux (nmol m^{-2} s^{-1})
2
1
0
-1
20 30 40 50 60 70 80 90
WFPS (%)
5 10 15
Soil Temperature (°C)
Site
Grassland
Woodland

292

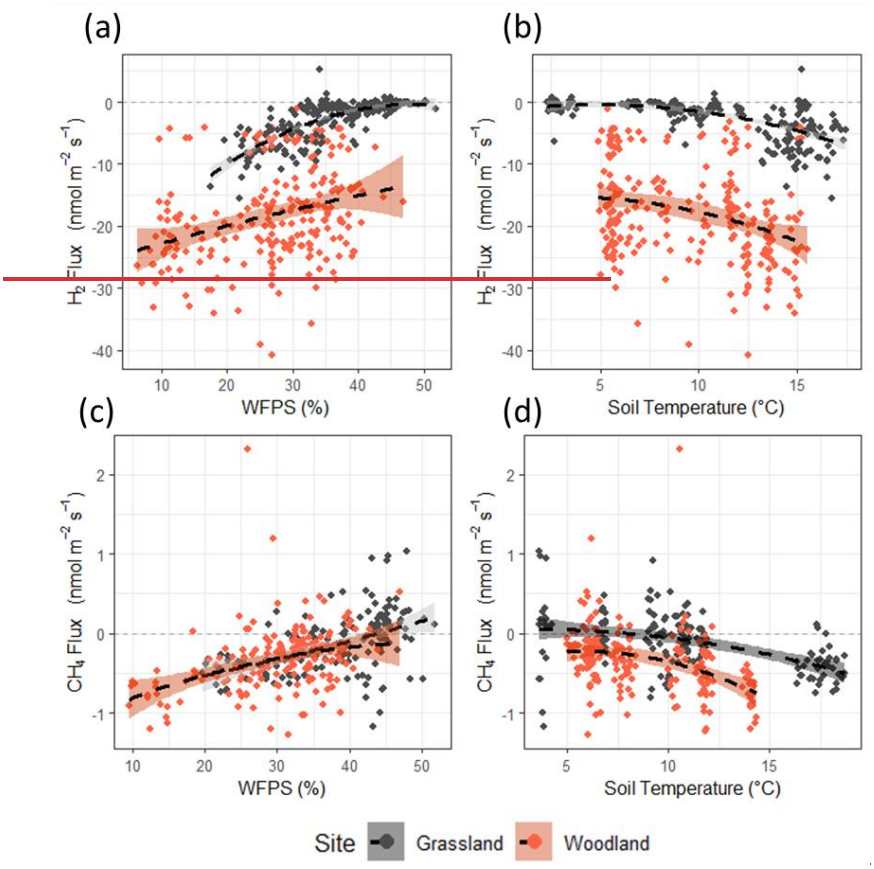

293

294

295 **Figure 3.** Correlations between H_2 flux and (a) water filled pore space (WFPS) and (b) Soil Temperature.
296 Correlations between CH_4 flux and (c) water filled pore space (WFPS) and (d) Soil Temperature. WFPS and soil
297 temperature measured at 10 cm depth via sampling probe. A 2nd order polynomial fit (black dashed line) is
298 included as a visual aid ($y = a_1x^2 + a_2x + c$) (Figure replicated for Vd in Figure S2).

299

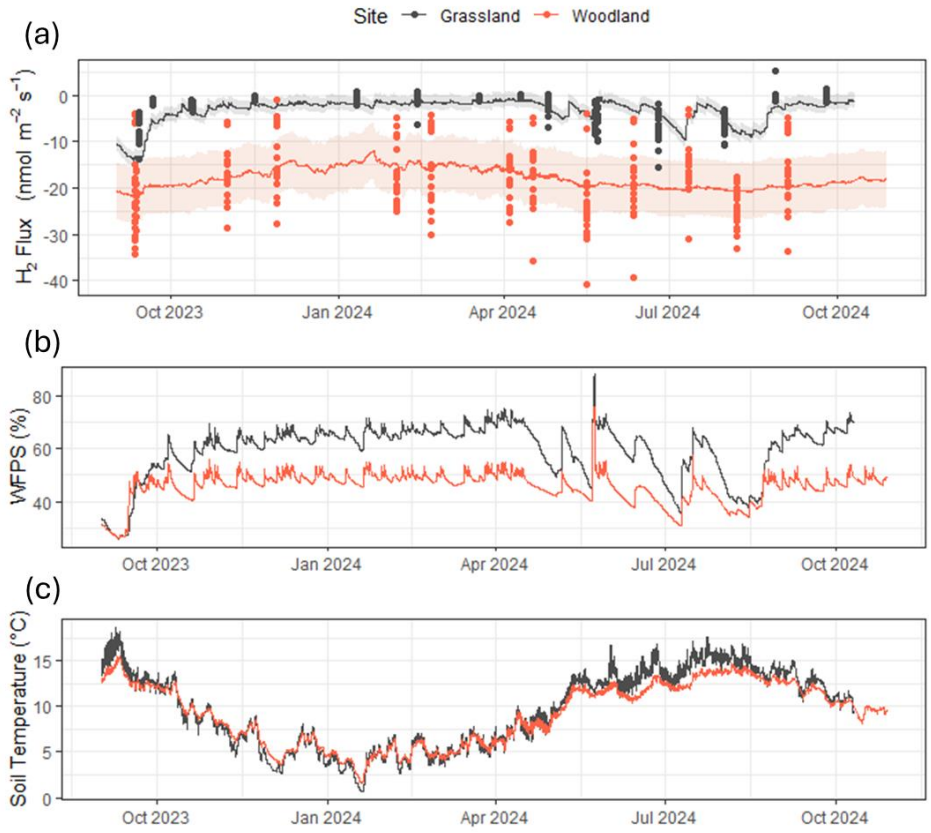
Site
Grassland
Woodland
(a)
H2 Flux (nmol m-2 s-1)
0
-10
-20
-30
-40
Oct 2023
Jan 2024
Apr 2024
Jul 2024
Oct 2024
(b)
WFPS (%)
80
60
40
Oct 2023
Jan 2024
Apr 2024
Jul 2024
Oct 2024
(c)
Soil Temperature (°C)
15
10
5
0
Oct 2023
Jan 2024
Apr 2024
Jul 2024
Oct 2024

300

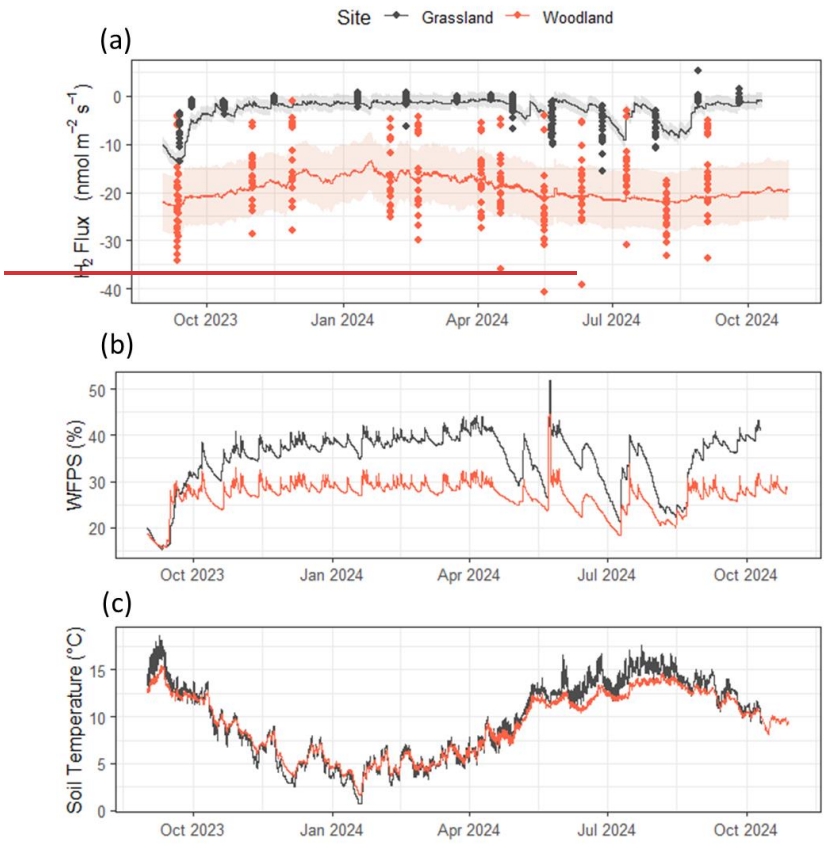

Figure 4. (a) H_2 flux measurements and model predictions for both field sites using a multiple regression fit with soil moisture (x) and soil temperature (z) ($y = a_1x^2 + a_2x + b_1z^2 + b_2z + c$). (b) Continuous water filled pore space (WFPS) at measurements made at 10 cm depth (average of 60 mins). (c) Continuous soil temperature at measurements made at 10 cm depth (average of 60 mins).

4. Discussion

4.1. Quantification of H_2 flux

Fluxes of H_2 measured in this study range from -40.7 to 5.3 nmol m^{-2} s^{-1} with mean fluxes of -2.6 ± 0.4 and -18.7 ± 1.0 nmol m^{-2} s^{-1} for the grassland and woodland sites, respectively. Using regression to model (gap-fill) flux data, we estimate annual H_2 uptake of 3.1 ± 0.1 and 12.0 ± 0.4 kg H_2 ha^{-1} yr^{-1} for the grassland and woodland sites, respectively, which increases the ~~expected~~ modelled mean uptake at the grassland site to 4.3 ± 0.2 nmol m^{-2} s^{-1} (in comparison to a measured mean uptake of 2.6 ± 0.4 nmol m^{-2} s^{-1}) while the expected mean uptake at the woodland site remains near 18 nmol m^{-2} s^{-1} (Table 3). Predicted uptake is higher at the grassland site due to the expectation in the model that uptake will increase during periods of drier soils that were not measured directly. Predicted uptake estimated by the model and the extrapolation of the mean flux are not significantly different at the woodland site due to the lack of correlation with soil drivers in the model. However, the model does predict that uptake will slow down during the coldest months when fewer measurements were made at the site.

Mean measured uptake of H_2 at the grassland site is at the lower end of uptake reported in other studies that directly measured H_2 flux from soils, which range from -1.5 to >20 nmol m^{-2} s^{-1} (Table 3). The mean soil uptake of H_2 at the woodland site is at the higher end in terms of uptake magnitude, close in magnitude to high deposition velocities reported for peatlands in Simmonds et al., (2011). While uptake at this site seems high, we are confident that the flux measurements are accurate based on the consistency of flux observations and the quality controls put in place. Concentrations of H_2 in the chambers consistently fell exponentially, reaching near zero within 5 minutes (often within 3 mins) of enclosure. At the time of chamber closure (t_o), a volume of 0.025 m^3 of ambient air at the woodland site contains approximately 400-500 nmol of H_2 gas. To reach zero within 5 mins would require fluxes approximately 10-12 nmol m^{-2} s^{-1} in magnitude. While dealing with the exponential non-linearity of the rate of change of the concentration (dC/dt) does introduce an element of uncertainty in the flux calculations, we are confident the method used in this study (HMR fitting) accurately captures the flux at t_o and thus a realistic magnitude of soil H_2 uptake.

Only two of the measured H_2 fluxes were both positive and larger than the analytical noise of the measurement method. However, these measurements from separate chambers on separate dates (from the grassland site) both showed 7 consecutive concentration measurements, all clearly increasing with time, highlighting that it is possible for H_2 emissions to occur in soils, even where uptake is the predominant direction of flux. It has been observed that legumes produce H_2 during the nitrogen fixation process (e.g. Schubert and Evans 1976; Flynn et al., 2014); however, no legume plants were present in any of the chamber locations during the study. The source of these H_2 emissions remains unknown and at no point did either of

the field sites become a source of H_2, but our observations do highlight that there remain unknown microbial and geological processes at the sub-field scale.

Table 43. A summary of H_2 net fluxes and deposition velocity (Vd) measurements reported in literature, compared with measured and modelled values in this study. Mean values and reported uncertainties. Where only flux or Vd is reported, missing values are estimated using an ambient H_2 concentration of 500 ppb.

Study	Soil Type	Country	Mean H_2 Flux (nmol m^{-2} s^{-1})	Mean Vd (cm s^{-1})
This study (measured)	Grass (Grazing)	UK (SCO)	-2.6 ± 0.4	0.012 ± 0.002
This study (gap-filled annual average)	Grass (Grazing)	UK (SCO)	-4.3 ± 0.2	
This study (measured)	Woodland	UK (SCO)	-18.2 ± 1.0	0.088 ± 0.005
This study (gap-filled annual average)	Woodland	UK (SCO)	-18.7 ± 0.6	
Smith-Downey et al. (2008)	Forest	USA (CA)	-7.9 ± 4.2	0.063 ± 0.029
	Desert	USA (CA)	-7.6 ± 5.3	0.051 ± 0.036
	Marsh	USA (CA)	-7.5 ± 3.4	0.035 ± 0.013
Lallo et al. (2009)	Urban park	FIN (Hesa)	-10.0 ± 2.5	0.020 ± 0.005
	Urban park	FIN (Hesa)	-19.0 ± 3.5	0.038 ± 0.007
Hammer and Levin (2009)	Urban/Agriculture	GER (BW)	-6.4 ± 1.6	0.03 ± 0.007
Simmonds et al. (2011)	Peatland	IRE (GAL)	-26.5 (-9.0 – -64.5)	0.053 (0.018 – 0.129)
Meredith et al. (2017)	Woodland	USA (MA)	-3.2 ± 1.6	0.003 to 0.043
Baril et al. (2022)	Arable	CAN (QC)	-5.9 ± 4.3	0.012 ± 0.009
Buzzard et al. (2022)	Desert (Monsoon)	USA (AZ)	-1.5 to -3.5	0.03 to 0.007
Nagai et al. (2024)	Arable	JAP (JP02)	-5 to -10	0.01 to 0.02

4.2. Drivers of H_2 flux

This study provides evidence of large variability in H_2 flux behaviour across two different soil types and the importance of environmental factors such as soil temperature and moisture content. At the grassland site, soil moisture (WFPS) dominated the net H_2 flux behaviour in the soils. The relationship between H_2 uptake and soil moisture was statistically significant ($p < 0.001$) and explained 60% of the variance observed in the grassland H_2 fluxes observed. While H_2 flux does appear to correlate with soil temperature at the grassland site when compared directly, this is almost entirely due to the strong correlation between soil moisture and soil temperature ($R^2 = 0.68$). Multiple regression finds soil temperature to be an insignificant variable once the effect of soil moisture is accounted for at the grassland site. Spatial variability in H_2 fluxes at the woodland site were an order of magnitude higher than those at the grassland site. This spatial variability could not be explained by soil moisture, temperature or the total carbon content of the soil. While there do appear to be

weak relationships between the flux data and soil moisture and soil temperature, neither is found to be statistically significant (maximum p-value of 0.15 for soil temperature).

Meteorological conditions were almost identical at the local scale (sites are less than 3 km apart) and soil at both sites was of a similar pH and had similar total carbon and nitrogen contents. A small difference in ambient H_2 concentrations was observed between the sites which may be caused by the large soil uptake and poorer circulation of air at the woodland site, resulting in lower near surface H_2 concentrations. The reason for the large difference in flux of H_2 measured between the two sites is not entirely clear from the measured data, but it is likely that the physical properties of the soils played a role. While rooting systems and carbon structure within the surface layers of the soils will be different at the sites, one large and obvious disparity is the silt/clay content of the soils which is approximately ~~55~~75% and ~~25~~40% at the grassland and woodland sites, respectively. While both soils have similar particle density, the difference in silt/clay content implies variations in pore size distribution and connectivity which will likely lead to different sensitivities to moisture changes. We hypothesise from this assessment that the high fraction of silt/clay soil at the grassland site results in the soil becoming highly anaerobic when moisture levels increase, as can be seen in the switching from CH_4 uptake to CH_4 emission when WFPS exceeded 40%. At the woodland site, a thin layer of organic materials (forest litter that could provide a source of labile carbon) lies on top of a sandy, well-drained soil, which may provide ideal conditions for H_2 uptake. Uptake of CH_4 is generally greater than at the grassland site, and WFPS remains lower throughout the year, showing that drainage is significantly faster at the site and suggests that the soils are more aerobic than at the grassland site (e.g. better penetration of H_2 to active regions within the soil). While the differences in soil texture may partly explain the large magnitude of difference in H_2 uptake between the sites, it does not account for the large spatial variability of H_2 flux at the woodland site. ~~While~~ We observe that the flux at the grassland site is largely dependent on physical factors at the field scale such as the moisture content (aeration) of the soil, but the woodland site showed large variations between plots. This variation may be due to microbial factors that are highly spatial in a forest floor, such as available nutrients (labile carbon from rotting plant litter), canopy shading and varying microbial densities.

4.3. Considerations for future research

Chamber flux methods are commonplace in the field of GHG flux measurements, but there are several important factors that need to be considered when carrying out H_2 flux measurements in the field. One of the most important - when using gas chromatography analysis - is the lifetime of samples stored in vials due to leakage rates from the rubber septum materials used to cap vials. While it is possible to keep GHG samples in these vials for weeks or even months without significant storage loss, H_2 concentrations were found to

change relatively quickly, and should be analysed as soon as is possible (within 24 h of measurement). This severely limits the reach of a particular field experiment to within travel distances of a working H_2 gas chromatography instrument (e.g. not suitable for international shipment of samples). Almost all published H_2 flux measurements to date are within the temperate region of the northern hemisphere (USA and Europe), which limits the available data for models to predict soil/atmosphere interactions at the global scale. Building H_2 flux datasets at a global level would require either investment in localised infrastructure that allows for samples to be analysed in-country, or for the deployment of temporary roving measurement methodology which travels between sites. We emphasise that unless particular care and attention is applied to the transportation of gas samples (e.g. tests and quality control checks), the H_2 flux cannot be analysed over a large distance due to leakage of samples.

Field measurements of H_2 are beneficial due to realistic environmental conditions. However, the manual aspects of chamber sampling create logistical issues (extensive fieldwork) and the overlap of many environmental and soil variables can make it difficult to identify the driving forces behind H_2 flux (e.g. the soil moisture/temperature comparison). With this setup, the GC-PDHID is limited to one gas sample every 4 minutes, thus auto-chambers (chambers that open/close and measure gas samples automatically) are limited in capability. New faster instruments able to measure H_2 gas via infra-red spectroscopy (by converting H_2 to H_2O) are becoming more commercially available (see aerodyne.com/laser-analyzers), but there are no studies using these analysers to date. Previously gas chromatography instrumentation has been used to measure H_2 flux via the aerodynamic gradient method (Meredith et al., 2017), which allows half hourly fluxes to be measured at the field scale. While micrometeorological methods such as the aerodynamic gradient method allow for a greater temporal and spatial coverage of soil fluxes, they also require certain field conditions, such as flat open terrain and large (mains) power supply. In the case of the woodland site in this study, micrometeorological methods are not feasible. With current available H_2 measurement methods, care must be given when planning measurement activities to ensure efficiency in data collection.

Lab-based incubation studies of H_2 flux in literature are similar in number to those measured in the field. Incubation studies allow for better control of soil conditions such as moisture, temperature and nutrient content, environmental conditions (air temperature) and also for consistency in microbial populations (via replicates of well mixed/homogenised soils). For example, in this study, it was difficult to determine the impact of soil temperature due to the correlation with soil moisture. Due to the climate in the region, there were no periods when the soils were cold and also dry, preventing observations of different extremes of the driving forces behind H_2 flux (see Figure S4). Incubation studies would be able to provide more information on these drivers which may help modelling efforts; however, field measurements are still required to validate flux models as incubation studies inevitably come with the caveat that flux measurements are not

representative of true soil conditions due to soil cores being repacked and creating therefore artificial conditions.

5. Conclusions

This study reports that the soil sink (uptake) of H_2 for a grassland and a forest site in close proximity is -3.1 ± 0.1 and -12.0 ± 0.4 kg H_2 ha^{-1} yr^{-1}, respectively (with mean Vds of 0.012 ± 0.002 and 0.088 ± 0.005 cm s^{-1} for grassland and forest soils, respectively). Soil moisture was found to be the primary driver of H_2 uptake at the grassland site, where the high silt/clay content of the soil resulted in anaerobic conditions (near zero H_2 flux) during wet periods of the year. Uptake of H_2 at the forest site was highly variable and did not correlate well with any localised soil properties. Both sites were exposed to similar meteorological conditions (3 km apart) and had similar basic soil properties (such as pH and carbon content), thus we conclude that the large difference in uptake between the soils was dependent on soil aeration and diffusivity of H_2. It is likely that the high silt/clay content of the grassland site (55%) resulted in a lack of aeration when soils were wet, while the well-drained forest site (25% clay) was not restricted by exchange of H_2 between the atmosphere and the soil, showing instead a large variability in H_2 flux that could be related to heterogeneous factors that control microbial activity (e.g. labile carbon and microbial densities). In order to account for the large magnitude of site-scale differences like those observed in this study, further field sites should be studied over a range of soil and land cover types and management activities to improve global models of the soil H_2 sink. In addition, laboratory incubations are needed to measure H_2 fluxes under controlled environmental conditions to refine the main driving parameters of H_2 fluxes further.

6. Acknowledgements

Funding for this study has been provided by the UKRI Natural Environment Research Council (NERC) under Grant Ref: NE/X013456/1 (Topic B: The Enigma of the Soil Hydrogen Sink Variability [ELGAR]). The work has also been supported by the UK Research and Innovation (UKRI) Global Challenges Research Fund (GCRF) as part of the South Asia Nitrogen Hub SANH project (NE/S009019/1).

7. Competing interests

The authors declare that they have no conflict of interest.

8. Data availability

Data currently undergoing preparation for submission to the Environmental Information Data Centre (EIDC). https://eidc.ac.uk/

9. Author contributions

N. Cowan was the primary author of the manuscript and carried out all data analysis presented. The field team that developed measurement methodology protocols, carried out measurements, maintained field instrumentation and performed lab analysis consisted of T. Roberts, M. Hanlon, A. Bezanger, G. Toteva, A. Tweedie, K. Yeung and A. Deshpande. The project management and significant contributors to the manuscript text consisted of P. Levy, U. Skiba, E. Nemitz and J. Drewer. All coauthors contributed to the writing of the manuscript before submission.

10. References

Baril, X., Durand, A.-A., Srei, N., Lamothe, S., Provost, C., Martineau, C., Dunfield, K., Constant, P., 2022. The biological sink of atmospheric H2 is more sensitive to spatial variation of microbial diversity than N_2O and CO_2 emissions in a winter cover crop field trial. Science of The Total Environment. https://doi.org/10.1016/j.scitotenv.2022.153420

Bertagni, M.B., Pacala, S.W., Paulot, F., Porporato, A., 2022. Risk of the hydrogen economy for atmospheric methane. Nat Commun. https://doi.org/10.1038/s41467-022-35419-7

Billington, H.L. and Pelham, J., 1991. Genetic Variation in the Date of Budburst in Scottish Birch Populations: Implications for Climate Change. Functional Ecology, 5(3), pp. 403–409. https://doi.org/10.2307/2389812.

Buzzard, V., Thorne, D., Gil-Loaiza, J., Cueva, A., Meredith, L.K., 2022. Sensitivity of soil hydrogen uptake to natural and managed moisture dynamics in a semiarid urban ecosystem. PeerJ. https://doi.org/10.7717/peerj.12966

~~Conrad, R., 1999. Contribution of hydrogen to methane production and control of hydrogen concentrations in methanogenic soils and sediments. FEMS Microbiology Ecology. https://doi.org/10.1111/j.1574-6941.1999.tb00575.x~~

478 Cooper, J., Dubey, L., Bakkaloglu, S., Hawkes, A., 2022. Hydrogen emissions from the hydrogen value chain-
479 emissions profile and impact to global warming. Science of The Total Environment.
480 https://doi.org/10.1016/j.scitotenv.2022.154624

481 Cowan, N., Levy, P., Maire, J., Coyle, M., Leeson, S.R., Famulari, D., Carozzi, M., Nemitz, E., Skiba, U., 2020. An
482 evaluation of four years of nitrous oxide fluxes after application of ammonium nitrate and urea fertilisers
483 measured using the eddy covariance method. Agricultural and Forest Meteorology.
484 https://doi.org/10.1016/j.agrformet.2019.107812

485 Cowan, N., Levy, P., Tigli, M., Toteva, G., Drewer, J., 2025. Characterisation of Analytical Uncertainty in
486 Chamber Soil Flux Measurements. European J Soil Science. https://doi.org/10.1111/ejss.70104

487 Derwent, R.G., Stevenson, D.S., Utembe, S.R., Jenkin, M.E., Khan, A.H., Shallcross, D.E., 2020. Global modelling
488 studies of hydrogen and its isotopomers using STOCHEM-CRI: Likely radiative forcing consequences of a
489 future hydrogen economy. International Journal of Hydrogen Energy.
490 https://doi.org/10.1016/j.ijhydene.2020.01.125

491 Deshpande, A.G., Jones, M.R., van Dijk, N., Mullinger, N.J., Harvey, D., Nicoll, R., Toteva, G., Weerakoon, G.,
492 Nissanka, S., Weerakoon, B., Grenier, M., Iwanicka, A., Duarte, F., Stephens, A., Ellis, C.J., Vieno, M., Drewer,
493 J., Wolseley, P.A., Nanayakkara, S., Prabhashwara, T., Bealey, W.J., Nemitz, E., Sutton, M.A., 2024.
494 Estimation of ammonia deposition to forest ecosystems in Scotland and Sri Lanka using wind-controlled
495 NH_3 enhancement experiments. Atmospheric Environment.
496 https://doi.org/10.1016/j.atmosenv.2023.120325

497 Drewer, J., Anderson, M., Levy, P.E., Scholtes, B., Helfter, C., Parker, J., Rees, R.M., Skiba, U.M., 2016. The
498 impact of ploughing intensively managed temperate grasslands on N2O, CH4 and CO2 fluxes. Plant Soil.
499 https://doi.org/10.1007/s11104-016-3023-x

500 Drewer, J., Anderson, M., Levy, P.E., Scholtes, B., Helfter, C., Parker, J., Rees, R.M., Skiba, U.M., 2016. The
501 impact of ploughing intensively managed temperate grasslands on N2O, CH4 and CO2 fluxes. Plant Soil.
502 https://doi.org/10.1007/s11104-016-3023-x

503 Ehhalt, D.H., Rohrer, F., 2009. The tropospheric cycle of H_2: a critical review. Tellus B: Chemical and Physical
504 Meteorology. https://doi.org/10.1111/j.1600-0889.2009.00416.x

505 Field, R.A., Derwent, R.G., 2021. Global warming consequences of replacing natural gas with hydrogen in the
506 domestic energy sectors of future low-carbon economies in the United Kingdom and the United States of
507 America. International Journal of Hydrogen Energy. https://doi.org/10.1016/j.ijhydene.2021.06.120

508 Flynn, B., Graham, A., Scott, N., Layzell, D.B., Dong, Z., 2014. Nitrogen fixation, hydrogen production and N_2O
509 emissions. Can. J. Plant Sci. https://doi.org/10.4141/cjps2013-210

510 Greening, C., Grinter, R., 2022. Microbial oxidation of atmospheric trace gases. Nat Rev Microbiol.
511 https://doi.org/10.1038/s41579-022-00724-x

512 Hammer, S., Levin, I., 2009. Seasonal variation of the molecular hydrogen uptake by soils inferred from
513 continuous atmospheric observations in Heidelberg, southwest Germany. Tellus B: Chemical and Physical
514 Meteorology. https://doi.org/10.1111/j.1600-0889.2009.00417.x

515 Hitchcock, W. K., Beamish, B. B. and Cliff D., 2019. A Study of the Formation of Hydrogen Produced During the
516 Oxidation of Bulk Coal Under Laboratory Conditions, in Naj Aziz and Bob Kininmonth (eds.), Proceedings
517 of the 2008 Coal Operators' Conference, Mining Engineering, University of Wollongong

518 Hutchinson, G.L., Mosier, A.R., 1981. Improved Soil Cover Method for Field Measurement of Nitrous Oxide
519 Fluxes. Soil Science Society of America Journal.
520 https://doi.org/10.2136/sssaj1981.03615995004500020017x

521 Islam, Z.F., Welsh, C., Bayly, K., Grinter, R., Southam, G., Gagen, E.J., Greening, C., 2020. A widely distributed
522 hydrogenase oxidises atmospheric H2 during bacterial growth. The ISME Journal.
523 https://doi.org/10.1038/s41396-020-0713-4

524 Khalil, M.A.K., Rasmussen, R.A., 1990. The global cycle of carbon monoxide: Trends and mass balance.
525 Chemosphere. https://doi.org/10.1016/0045-6535(90)90098-e

526 Field, R.A., Derwent, R.G., 2021. Global warming consequences of replacing natural gas with hydrogen in the
527 domestic energy sectors of future low-carbon economies in the United Kingdom and the United States of
528 America. International Journal of Hydrogen Energy. https://doi.org/10.1016/j.ijhydene.2021.06.120

529 Lallo, M., Aalto, T., Hatakka, J., Laurila, T., 2009. Hydrogen soil deposition at an urban site in Finland. Atmos.
530 Chem. Phys. https://doi.org/10.5194/acp-9-8559-2009

531 Meredith, L.K., Commane, R., Keenan, T.F., Klosterman, S.T., Munger, J.W., Templer, P.H., Tang, J., Wofsy, S.C.,
532 Prinn, R.G., 2016. Ecosystem fluxes of hydrogen in a mid-latitude forest driven by soil microorganisms and
533 plants. Global Change Biology. https://doi.org/10.1111/gcb.13463

534 Nagai, M., Kakiuchi, H., Masuda, T., 2024. Measurements of hydrogen deposition velocities by farmland soil
535 using D2 gas. Radiation Protection Dosimetry. https://doi.org/10.1093/rpd/ncae055

536 Novelli, P.C., Lang, P.M., Masarie, K.A., Hurst, D.F., Myers, R., Elkins, J.W., 1999. Molecular hydrogen in the
537 troposphere: Global distribution and budget. J. Geophys. Res. https://doi.org/10.1029/1999jd900788

538 Ocko, I.B., Hamburg, S.P., 2022. Climate consequences of hydrogen emissions. Atmos. Chem. Phys.
539 https://doi.org/10.5194/acp-22-9349-2022

540 Paulot, F., Paynter, D., Naik, V., Malyshev, S., Menzel, R., Horowitz, L.W., 2021. Global modeling of hydrogen
541 using GFDL-AM4.1: Sensitivity of soil removal and radiative forcing. International Journal of Hydrogen
542 Energy. https://doi.org/10.1016/j.ijhydene.2021.01.088

543 Paulot, F., Pétron, G., Crotwell, A.M., Bertagni, M.B., 2024. Reanalysis of NOAA H2 observations: implications
544 for the H2 budget. Atmos. Chem. Phys. https://doi.org/10.5194/acp-24-4217-2024

545 Patterson, J.D., Aydin, M., Crotwell, A.M., Pétron, G., Severinghaus, J.P., Krummel, P.B., Langenfelds, R.L.,
546 Saltzman, E.S., 2021. H 2 in Antarctic firn air: Atmospheric reconstructions and implications for
547 anthropogenic emissions. Proc. Natl. Acad. Sci. U.S.A. https://doi.org/10.1073/pnas.2103335118

548 Pedersen, A.R., Petersen, S.O., Schelde, K., 2010. A comprehensive approach to soil-atmosphere trace-gas
549 flux estimation with static chambers. European J Soil Science. https://doi.org/10.1111/j.1365-
550 2389.2010.01291.x

551 Petron, G. B., Crotwell, A. M., Mund, J., Crotwell, M., Mefford, T., Thoning, K., Hall, B. D., Kitzis, D. R.,
552 Madronich, M., Moglia, E., Neff, D., Wolter, S., Jordan, A., Krummel, P., Langenfelds, R., and Patterson, J.
553 D.: Atmospheric H2 observations from the NOAA Global Cooperative Air Sampling Network, Atmos. Meas.
554 Tech. Discuss. [preprint], https://doi.org/10.5194/amt-2024-4, in review, 2024.

555 Piché-Choquette, S., Constant, P., 2019. Molecular Hydrogen, a Neglected Key Driver of Soil Biogeochemical
556 Processes. Appl Environ Microbiol. https://doi.org/10.1128/aem.02418-18

557 Saavedra-Lavoie, J., de la Porte, A., Piché-Choquette, S., Guertin, C., Constant, P., 2020. Biological H2 and CO
558 oxidation activities are sensitive to compositional change of soil microbial communities. Can. J. Microbiol.
559 https://doi.org/10.1139/cjm-2019-0412

560 Sand, M., Skeie, R.B., Sandstad, M., Krishnan, S., Myhre, G., Bryant, H., Derwent, R., Hauglustaine, D., Paulot,
561 F., Prather, M., Stevenson, D., 2023. A multi-model assessment of the Global Warming Potential of
562 hydrogen. Commun Earth Environ. https://doi.org/10.1038/s43247-023-00857-8

563 Schubert, K.R., Evans, H.J., 1976. Hydrogen evolution: A major factor affecting the efficiency of nitrogen
564 fixation in nodulated symbionts. Proc. Natl. Acad. Sci. U.S.A. https://doi.org/10.1073/pnas.73.4.1207

565 Simmonds, P.G., Derwent, R.G., Manning, A.J., Grant, A., O'doherty, S., Spain, T.G., 2011. Estimation of
566 hydrogen deposition velocities from 1995–2008 at Mace Head, Ireland using a simple box model and

concurrent ozone depositions. Tellus B: Chemical and Physical Meteorology. https://doi.org/10.1111/j.1600-0889.2010.00518.x

Smith-Downey, N.V., Randerson, J.T., Eiler, J.M., 2008. Molecular hydrogen uptake by soils in forest, desert, and marsh ecosystems in California. J. Geophys. Res. https://doi.org/10.1029/2008jg000701

Warwick, N.J., Bekki, S., Nisbet, E.G., Pyle, J.A., 2004. Impact of a hydrogen economy on the stratosphere and troposphere studied in a 2-D model. Geophysical Research Letters. https://doi.org/10.1029/2003gl019224